

## A semi-analytical approach for stress concentration of cantilever beams with circular holes under bending

### 半解析法求解懸臂梁受彎矩之應力集中問題

Po-Yuan Chen<sup>1</sup> and Jeng-Tzong Chen<sup>2</sup>

<sup>1</sup>Graduate Student, Department of Harbor and River Engineering

<sup>2</sup>Distinguished Professor, Department of Harbor and River Engineering

National Taiwan Ocean University

#### Abstract

In the paper, the degenerate kernels and Fourier series expansions are adopted in the null-field integral equation to solve bending problems of a circular beam with circular holes. The main gain of using degenerate kernels in integral equations is free of calculating the principal values for singular integrals. An adaptive observer system is addressed to fully employ the property of degenerate kernels for circular boundaries in the polar coordinate. After moving the null-field point to the boundary and matching the boundary conditions, a linear algebraic system is obtained without boundary discretization. The present method is treated as a “semi-analytical” since analytical expressions as much as possible before numerical implementation. Finally, an example, including four holes, is given to demonstrate the validity of the proposed method. The present formulation can be extended to handle beam problems with arbitrary number and various positions of circular holes.

**Keywords:** Null-field integral equation; degenerate kernel; Fourier series; circular holes; cantilever beam; stress concentration

#### 摘要

本文利用退化核及傅立葉級數展開搭配零場積分方程求解圓形斷面梁含圓型孔洞的彎曲問題。藉由分離核函數的表示式，可免於計算邊界積分中計算主值的困擾。文中採用自適性觀察座標系統來充分掌握分離核函數的特性。透過零場積分方程將零場點推向邊界，滿足邊界條件後可以得到線性代數方程式，其中未知的傅立葉係數可輕易地求得。本法可稱之為“半解析”法，其主要誤差來源為所截取的傅立葉項數。最後，以一個包含四個圓孔洞的例子來驗證此方法的正確性，且探討應力集中發生之位置。藉由此方法可進行任意個數及不同位置之孔洞的彎矩分析。

**關鍵字:**零場積分方程；退化核；傅立葉級數；圓孔；懸臂梁；應力集中

## Introduction

The stress concentration around holes of a beam under bending or torsion plays an important role in promoting the design criteria for higher factors of safety. Those problems have been visited in a few investigations based on the Saint-Venant theory<sup>1,2</sup>. For a simple case, an analytical solution may be available. Since the analytical solution for more than two holes may encounter difficulty, several numerical approaches have been employed, *e.g.* complex variable boundary element method (CVBEM) by Chou<sup>3</sup> and Ang and Kang<sup>4</sup>. The CVBEM was primarily introduced by Hromadka and Lai<sup>5</sup> for solving the Laplace problems in an infinite domain. In 1997, Chou<sup>3</sup> extended the work of Hromadka to multiply-connected problems. Recently, Ang and Kang<sup>4</sup> developed a general formulation for solving the second-order elliptic partial differential equation for a multiply-connected region in a different version of CVBEM. The Cauchy integral formulae are offered to solve the boundary value problem. By introducing the CVBEM, Chou<sup>3</sup> and Ang and Kang<sup>4</sup> have revisited the anti-plane problems with two circular holes whose centers lie on the  $x$  axis investigated by Honein *et al.*<sup>6</sup>. In 1991, Naghdi<sup>7</sup> employed a special class of basic function, which is the Saint-Venant flexure function suitable for the problem of the bending of a circular cylinder with  $4N$  ( $N=1,2,3,\dots$ ) circular holes in the axial direction. Bird and Steele<sup>8</sup> used the Fourier series procedure to revisit the antiplane problems in the Honein's paper<sup>6</sup>. Also, they solved the bending problems which were solved by Naghdi<sup>7</sup>. In the literature, it is observed that exact solutions for boundary value problems are only limited for simple cases. Although Naghdi<sup>7</sup> has proposed a solution for bending problems with holes, it is limited to  $4N$  ( $N=1,2,3,\dots$ ) holes. Therefore, proposing a systematic approach for solving BVP with various numbers of circular boundaries and arbitrary positions and radii is our goal in this paper. Following the success of anti-plane problems with circular holes<sup>9</sup>, the null-field integral equation is utilized to solve the Saint-Venant bending problem of a beam with circular holes. The mathematical formulation is derived by using degenerate kernels for fundamental solutions and Fourier series for boundary densities in formulation. Then, it reduces to a linear algebraic equation by using collocation approach. After determining the unknown coefficients, series solution for the bending function is obtained. The location of maximum stress concentration factor (SCF) is addressed. Numerical examples are given to show the validity and efficiency of our approach.

## Problem statement

Consider a beam with a circular section weakened by four circular holes placed on a concentric ring of radius  $a$  as show in Fig. 1. The radii of outer circle and inner holes are  $R$  and  $b$ , respectively. The beam is subject to a shear force  $Q$  at the free end, and the boundary conditions of outer circle and inner holes are traction free. Following the theory of

Saint-Venant bending, we assume the stress to be

$$\sigma_{xx} = \sigma_{yy} = \sigma_{xy} \equiv 0, \quad \sigma_{zz} = -\frac{Q}{I_y} x(l-z), \quad (1)$$

where  $I_y$  is the moment of inertia of beam cross section for the  $y$ -axis. The other two stress components are assumed as

$$\sigma_{zx} = \alpha\mu \left( \frac{\partial\varphi}{\partial x} + y \right) - \frac{Q}{2(1+\nu)I_y} \left[ \frac{\partial\psi}{\partial x} + \frac{1}{2}\nu x^2 + \left(1 - \frac{1}{2}\nu\right)y^2 \right], \quad (2)$$

$$\sigma_{zy} = \alpha\mu \left( \frac{\partial\varphi}{\partial y} + x \right) - \frac{Q}{2(1+\nu)I_y} \left[ \frac{\partial\psi}{\partial y} + (2+\nu)xy \right], \quad (3)$$

where  $\varphi(x, y)$  and  $\psi(x, y)$  are the warping function and bending function of the beam, respectively, and  $\alpha\mu$  is a constant. Since the  $\varphi(x, y)$  and  $\psi(x, y)$  in the Saint-Venant bending problem satisfies the two Laplace equations subject to the Neumann boundary condition, we have:

$$\nabla^2\varphi(x, y) = \frac{\partial^2\varphi}{\partial x^2} + \frac{\partial^2\varphi}{\partial y^2} = 0 \quad \text{in } D, \quad (4)$$

$$\frac{\partial\varphi}{\partial n} = y \cos(n, x) - x \cos(n, y) \quad x, y \in B_i, \quad (5)$$

and

$$\nabla^2\psi(x, y) = \frac{\partial^2\psi}{\partial x^2} + \frac{\partial^2\psi}{\partial y^2} = 0 \quad \text{in } D, \quad (6)$$

$$\frac{\partial\psi}{\partial n} = -\left[ \frac{1}{2}\nu x^2 + \left(1 - \frac{1}{2}\nu\right)y^2 \right] \cos(n, x) - (2+\nu)xy \cos(n, y) \quad x, y \in B_k, \quad (7)$$

where  $D$  is the domain of interest,  $n$  is the outward normal vector of each boundary, and  $B_k$  is the  $k$ th circular boundary. In Fig. 1, we define the position vector  $(x_k, y_k)$  of the boundary point on the  $i$ th circular boundary as

$$x_k = b \cos \theta_k + Dx_k, \quad k = 0, 1, 2, 3, 4, \quad 0 < \theta_k < 2\pi \quad (8)$$

$$y_k = b \sin \theta_k + Dy_k, \quad k = 0, 1, 2, 3, 4, \quad 0 < \theta_k < 2\pi \quad (9)$$

where  $(Dx_k, Dy_k)$  is the coordinate for the center of the  $k$ th eccentric circle, and the eccentricity is zero for the outer circle. By substituting Eqs. (8) and (9) into Eq. (7), the boundary condition is specified.

For the simple case of bending only, we can assume constant  $\alpha\mu$  and  $\psi(x, y)$  to be zero. Following the definition of stress concentration by Naghdi<sup>7</sup>, we have

$$Sc = \frac{\sigma_{zx} A}{Q}, \quad (10)$$

where  $A$  is the area of the cross-section. The shear stress  $\sigma_{zx}$  in Eq. (10) is obtained from the Eq. (2). Thus, the problem of bending is reduced to find the bending function  $\psi(x, y)$  which satisfies the Laplace equation of Eq. (6) and the Neumann boundary condition of Eq. (7) on each boundary.

## Dual boundary integral equations and dual null-field integral equations

Employing the Fourier series expansions to approximate the potential  $u$  and its normal derivative  $t$  on the circular boundary

$$u(s_k) = a_0^k + \sum_{n=1}^{\infty} (a_n^k \cos n\theta_k + b_n^k \sin n\theta_k), \quad s_k \in B_k, \quad k = 1, 2, \dots, N, \quad (11)$$

$$t(s_k) = p_0^k + \sum_{n=1}^{\infty} (p_n^k \cos n\theta_k + q_n^k \sin n\theta_k), \quad s_k \in B_k, \quad k = 1, 2, \dots, N, \quad (12)$$

where  $t(s_k) = \partial u(s_k) / \partial n_s$  in which  $n_s$  denotes the outward normal vector at the source point  $s$ ,  $a_n^k$ ,  $b_n^k$ ,  $p_n^k$  and  $q_n^k$  ( $n = 0, 1, 2, \dots$ ) are the Fourier coefficients and  $\theta_k$  is the polar angle for the  $k$ th circular boundary. The integral equation for the domain point can be derived from the third Green's identity<sup>10</sup>, as shown below:

$$2\pi u(x) = \int_B T(s, x) u(s) dB(s) - \int_B U(s, x) t(s) dB(s), \quad x \in D, \quad (13)$$

$$2\pi t(x) = \int_B M(s, x) u(s) dB(s) - \int_B L(s, x) t(s) dB(s), \quad x \in D, \quad (14)$$

where  $s$  and  $x$  are the source and field points, respectively,  $B$  is the boundary,  $D$  is the domain of interest, and the kernel function  $U(s, x) = \ln r$ , ( $r \equiv |x - s|$ ), is the fundamental solution which satisfies

$$\nabla^2 U(s, x) = 2\pi \delta(x - s), \quad (15)$$

in which  $\delta(x - s)$  denotes the Dirac-delta function. The other kernel functions,  $T(s, x)$ ,  $L(s, x)$  and  $M(s, x)$ , are defined by

$$T(s, x) \equiv \frac{\partial U(s, x)}{\partial n_s}, \quad L(s, x) \equiv \frac{\partial U(s, x)}{\partial n_x}, \quad M(s, x) \equiv \frac{\partial^2 U(s, x)}{\partial n_s \partial n_x}, \quad (16)$$

By collocating  $x$  outside the domain ( $x \in D^c$ ), we obtain the dual null-field integral equations as shown below

$$0 = \int_B T(s, x) u(s) dB(s) - \int_B U(s, x) t(s) dB(s), \quad x \in D^c, \quad (17)$$

$$0 = \int_B M(s, x) u(s) dB(s) - \int_B L(s, x) t(s) dB(s), \quad x \in D^c, \quad (18)$$

where  $D^c$  is the complementary domain. Based on the separable property, the kernel function  $U(s, x)$  is expanded into the degenerate form by separating the source point and field point in the polar coordinate:

$$U(s, x) = \begin{cases} U^i(R, \theta; \rho, \phi) = \ln R - \sum_{m=1}^{\infty} \frac{1}{m} \left(\frac{\rho}{R}\right)^m \cos m(\theta - \phi), & R \geq \rho \\ U^e(R, \theta; \rho, \phi) = \ln \rho - \sum_{m=1}^{\infty} \frac{1}{m} \left(\frac{R}{\rho}\right)^m \cos m(\theta - \phi), & \rho > R \end{cases}, \quad (19)$$

where the superscripts “*i*” and “*e*” denote the interior ( $R > \rho$ ) and exterior ( $\rho > R$ ) cases, respectively. After taking the normal derivative with respect to Eq. (19), the  $T(s, x)$  kernel function yields

$$T(s, x) = \begin{cases} T^i(R, \theta; \rho, \phi) = \frac{1}{R} + \sum_{m=1}^{\infty} \left( \frac{\rho^m}{R^{m+1}} \right) \cos m(\theta - \phi), & R > \rho \\ T^e(R, \theta; \rho, \phi) = -\sum_{m=1}^{\infty} \left( \frac{R^{m-1}}{\rho^m} \right) \cos m(\theta - \phi), & \rho > R \end{cases}, \quad (20)$$

and the higher-order kernel functions,  $L(s, x)$  and  $M(s, x)$ , are shown below:

$$L(s, x) = \begin{cases} L^i(R, \theta; \rho, \phi) = -\sum_{m=1}^{\infty} \left( \frac{\rho^{m-1}}{R^m} \right) \cos m(\theta - \phi), & R > \rho \\ L^e(R, \theta; \rho, \phi) = \frac{1}{\rho} + \sum_{m=1}^{\infty} \left( \frac{R^m}{\rho^{m+1}} \right) \cos m(\theta - \phi), & \rho > R \end{cases}, \quad (21)$$

$$M(s, x) = \begin{cases} M^i(R, \theta; \rho, \phi) = \sum_{m=1}^{\infty} \left( \frac{m\rho^{m-1}}{R^{m+1}} \right) \cos m(\theta - \phi), & R \geq \rho \\ M^e(R, \theta; \rho, \phi) = \sum_{m=1}^{\infty} \left( \frac{mR^{m-1}}{\rho^{m+1}} \right) \cos m(\theta - \phi), & \rho > R \end{cases}. \quad (22)$$

Since the potentials resulted from  $T(s, x)$  and  $L(s, x)$  are discontinuous cross the boundary, the potentials of  $T(s, x)$  and  $L(s, x)$  for  $R \rightarrow \rho^+$  and  $R \rightarrow \rho^-$  are different. This is the reason why  $R = \rho$  is not included in the expression for the degenerate kernels of  $T(s, x)$  and  $L(s, x)$  in Eqs. (20) and (21).

### Adaptive observer system

After moving the null-field point of Eq. (17) to the boundary, the boundary integrals through all the circular contours are required to be calculated. Since the boundary integral equations are frame indifferent due to the energy or work form, namely, objectivity rule, the observer system is adaptively to locate the origin at the center of circle under integration. Adaptive observer system is chosen to fully employ the property of degenerate kernels. The origin of the observer system is located on the center of the corresponding circle under integration to entirely utilize the geometry of circular boundary for the expansion of degenerate kernels and boundary densities.

### Vector decomposition technique of the potential gradient for the stress calculation in the hypersingular formulation

Equation (12) shows the normal derivative of potential for domain points, special treatment is considered here. Not only for calculating the stress but also for degenerate scales<sup>11</sup>, potential gradient on the boundary using hypersingular formulation is required to calculate. For the non-concentric case, special treatment for the normal derivative should be

taken care as the source point and field point locate on different circular boundaries. As shown in Fig. 2, the normal direction on the boundary (1, 1') should be superimposed by the radial derivative (3, 3') and angular derivative (4, 4'). We called this treatment "vector decomposition technique". According to the concept of vector decomposition technique,  $L(s, x)$  and  $M(s, x)$  in Eqs. (21) and (22) can be rewritten as shown bellow

$$L(s, x) = \begin{cases} L^i(R, \theta; \rho, \phi) = -\sum_{m=1}^{\infty} \left(\frac{\rho^{m-1}}{R^m}\right) \cos m(\theta - \phi) \cos(\zeta - \xi) \\ \quad - \sum_{m=1}^{\infty} \left(\frac{\rho^{m-1}}{R^m}\right) \sin m(\theta - \phi) \cos\left(\frac{\pi}{2} - \zeta + \xi\right), R > \rho \\ L^e(R, \theta; \rho, \phi) = \frac{1}{\rho} + \sum_{m=1}^{\infty} \left(\frac{R^m}{\rho^{m+1}}\right) \cos m(\theta - \phi) \cos(\zeta - \xi) \\ \quad - \sum_{m=1}^{\infty} \left(\frac{R^m}{\rho^{m+1}}\right) \sin m(\theta - \phi) \cos\left(\frac{\pi}{2} - \zeta + \xi\right), \rho > R \end{cases}, \quad (23)$$

$$M(s, x) = \begin{cases} M^i(R, \theta; \rho, \phi) = \sum_{m=1}^{\infty} \left(\frac{m\rho^{m-1}}{R^{m+1}}\right) \cos m(\theta - \phi) \cos(\zeta - \xi) \\ \quad - \sum_{m=1}^{\infty} \left(\frac{m\rho^{m-1}}{R^{m+1}}\right) \sin m(\theta - \phi) \cos\left(\frac{\pi}{2} - \zeta + \xi\right), R \geq \rho \\ M^e(R, \theta; \rho, \phi) = \sum_{m=1}^{\infty} \left(\frac{mR^{m-1}}{\rho^{m+1}}\right) \cos m(\theta - \phi) \cos(\zeta - \xi) \\ \quad - \sum_{m=1}^{\infty} \left(\frac{mR^{m-1}}{\rho^{m+1}}\right) \sin m(\theta - \phi) \cos\left(\frac{\pi}{2} - \zeta + \xi\right), \rho > R \end{cases}, \quad (24)$$

where  $\zeta$  and  $\xi$  are shown in Fig. 2. For the concentric case, the circles with respect to the same origin of observer, the potential gradient is derived free of special treatment since  $\zeta = \xi$ .

### Linear algebraic system

We need to collocate  $2M + 1$  null-field point on the boundary to calculate  $2M + 1$  unknown Fourier coefficients. By moving the null-field point  $x_k$  on the  $k$ th circular boundary in the sense of limit for Eq. (17), we have

$$0 = \sum_{k=1}^{N_c} \int_{B_k} T(s_k, x_j) u(s_k) dB_k(s) - \sum_{k=1}^{N_c} \int_{B_k} U(s_k, x_j) t(s_k) dB_k(s), \quad x \in D^c, \quad (25)$$

where  $N_c$  is the number of circles including the outer boundary and the inner circular holes. If the domain is unbounded, the outer boundary  $B_0$  is a null set and  $N_c = N$ . By moving the null-field point on the boundary, a linear algebraic system is obtained

$$[\mathbf{U}]\{\mathbf{t}\} = [\mathbf{T}]\{\mathbf{u}\}, \quad (26)$$

where  $[\mathbf{U}]$  and  $[\mathbf{T}]$  are the influence matrices with a dimension of  $N_c(2M + 1)$  by  $N_c(2M + 1)$ ,  $\{\mathbf{u}\}$  and  $\{\mathbf{t}\}$  denote the column vectors of Fourier coefficients with a

dimension of  $N_c(2M+1)$  by 1 in which  $[\mathbf{U}]$ ,  $[\mathbf{T}]$ ,  $\{\mathbf{u}\}$  and  $\{\mathbf{t}\}$  can be defined as follows:

$$[\mathbf{U}] = \begin{bmatrix} \mathbf{U}_{00} & \mathbf{U}_{01} & \cdots & \mathbf{U}_{0N} \\ \mathbf{U}_{10} & \mathbf{U}_{11} & \cdots & \mathbf{U}_{1N} \\ \vdots & \vdots & \ddots & \vdots \\ \mathbf{U}_{N0} & \mathbf{U}_{N1} & \cdots & \mathbf{U}_{NN} \end{bmatrix}, [\mathbf{T}] = \begin{bmatrix} \mathbf{T}_{00} & \mathbf{T}_{01} & \cdots & \mathbf{T}_{0N} \\ \mathbf{T}_{10} & \mathbf{T}_{11} & \cdots & \mathbf{T}_{1N} \\ \vdots & \vdots & \ddots & \vdots \\ \mathbf{T}_{N0} & \mathbf{T}_{N1} & \cdots & \mathbf{T}_{NN} \end{bmatrix}, \quad (27)$$

$$\{\mathbf{u}\} = \begin{bmatrix} \mathbf{u}_0 \\ \mathbf{u}_1 \\ \mathbf{u}_2 \\ \vdots \\ \mathbf{u}_N \end{bmatrix}, \quad \{\mathbf{t}\} = \begin{bmatrix} \mathbf{t}_0 \\ \mathbf{t}_1 \\ \mathbf{t}_2 \\ \vdots \\ \mathbf{t}_N \end{bmatrix}, \quad (28)$$

where the vectors  $\{\mathbf{u}_k\}$  and  $\{\mathbf{t}_k\}$  are in the form of  $\{a_0^k \ a_1^k \ b_1^k \ \cdots \ a_M^k \ b_M^k\}^T$  and  $\{p_0^k \ p_1^k \ q_1^k \ \cdots \ p_M^k \ q_M^k\}^T$ , respectively; the first subscript “ $j$ ” ( $j=0,1,2,\dots,N$ ) in  $[\mathbf{U}_{jk}]$  and  $[\mathbf{T}_{jk}]$  denotes the index of the  $j$ th circle where the collocation point is located and the second subscript “ $k$ ” ( $k=0,1,2,\dots,N$ ) denotes the index of the  $k$ th circle where the boundary data  $\{\mathbf{u}_k\}$  or  $\{\mathbf{t}_k\}$  are specified,  $M$  indicates the truncated terms of Fourier series. By rearranging the known and unknown sets, the unknown Fourier coefficients are determined. Equation (17) can be calculated by employing the orthogonal property of Fourier bases in the real computation. Only the finite  $M$  terms are used in the summation of Eqs. (11) and (12). After obtaining the unknown Fourier coefficients, the boundary stress and interior potential can be easily calculated.

### Illustrative examples and discussions

#### *Four circular holes*<sup>7,8,12</sup>

In order to check the validity of the present formulation, the Naghdi's beam problems<sup>7</sup> with four holes symmetrically located with respect to the  $x$  and  $y$  axis were revisited. All the numerical results were obtained by using ten terms of Fourier series ( $M=10$ ). We set the value of Poisson's ratio  $\nu=0.3$  and  $R=1$ . In Figs. 3(a) and 3(b), the values of the stress concentration  $Sc$  along  $AB$  and  $CD$  (as Fig. 1) are plotted versus the position  $\bar{Y}_1=17Y_1/AB$ , and  $\bar{Y}_2=17Y_2/CD$ , respectively. Figure 3(c) shows the stress concentration  $Sc$  along  $OT$ , and the  $\xi_1=18 \times OT$  for the case of  $a=0.5$ ,  $\bar{\theta}=\pi/4$  and  $b=0.1$ . Figures 3 (a) and 3(b) show that the maximum  $Sc$  occurs at  $B$  and  $C$  on the boundaries, respectively. For the  $Sc$  along  $OT$  in Figure 3(c), the maximum  $Sc$  occurs at the position near the center of the two above holes. Good agreement is made after comparing with the Naghdi's results<sup>7</sup>. In the literature, Naghdi<sup>7</sup> and Bird and Steele<sup>8</sup> also calculated the stress concentration factor at the point  $B$  for  $b=0.12$  and different values of  $a$ , Bird and Steele<sup>7</sup> stated that the deviation by the Naghdi's data is 11%. The grounds for this discrepancy were not identified in

their paper. Our numerical results are more agreeable to the Naghdi's data<sup>7</sup> as shown in Figs. 4, where Fig. 4(c) and 4(f) was not provided by Bird and Steele<sup>8</sup>.

## Conclusions

For the bending problem with circular holes, we have proposed a BIEM formulation by using degenerate kernels, null-field integral equation and Fourier series in companion with adaptive observer systems and vector decomposition. This method is a semi-analytical approach since only truncation error in the Fourier series is involved. An advantage of the method over Naghdi's approach<sup>7</sup> is that the extension to multiple circular holes of arbitrary radii and positions is straightforward. Results obtained by the present approach matched well with those of Naghdi's<sup>7</sup> although Bird and Steele's data<sup>8</sup> seems to deviate. Although only four holes were tested to compare with the Naghdi's<sup>7</sup> and Bird and Steele's results<sup>8</sup>, our general-purpose program can solve problems with arbitrary number and various positions of circular holes.

## References

1. Sokolnikoff, I.S., "Mathematical Theory of Elasticity", McGraw-Hill, New York (1956).
2. Timoshenko, S.P. and Goodier, J.N., "Theory of Elasticity", McGraw-Hill, New York (1970).
3. Chou, S.I., "Stress field around holes in antiplane shear using complex variable boundary element method", ASME Journal of Applied Mechanics. Vol. 64, pp. 432-435 (1997).
4. Ang, W.T. and Kang, I., "A complex variable boundary element method for elliptic partial differential equations in a multiply-connected region", International Journal of Computer Mathematics", Vol. 75, pp. 515-525 (2000).
5. Hromadka, T.V. and Lai, C., "The complex variable boundary element method in engineering analysis", Springer-Verlag, New York (1986).
6. Honein, E., Honein, T. and Herrmann, G., "Further aspects of the elastic field for two circular inclusions in antiplane elastostatics", ASME Journal of Applied Mechanics, Vol. 59, pp. 774-779 (1992).
7. Naghdi, A.K. "Bending of a Perforated Circular Cylindrical Cantilever", International Journal of Solids and Structures. Vol. 28 (6), pp. 739-749 (1991).
8. Bird, M.D., Steele, C.R., "A Solution Procedure for Laplace's Equation on Multiply Connected Circular Domains", ASME Journal of Applied Mechanics, Vol. 59, pp. 398-404(1992).
9. Chen, J.T., Shen, W.C. Wu, A.C., "Null-field Integral Equations for Stress Field around Circular Holes under Anti-plane Shear", Engineering Analysis with Boundary Elements. Vol. 30, pp. 205-217 (2006).
10. Chen, J.T., Hong, H.-K. "Review of Dual Boundary Element Methods with Emphasis on Hypersingular Integrals and Divergent Series", Applied Mechanics Reviews, ASME, Vol.

- 52, pp. 17-33 (1999).
11. Chen, J.T., Kuo, S.R. and Lin, J.H., "Analytical Study and Numerical Experiments for Degenerate Scale Problems in the Boundary Element Method for Two-dimensional Elasticity", *International Journal for Numerical Methods in Engineering*, Vol. 54, pp. 1669-1681 (2002).
  12. Bird, M.D. "A Fourier Series Method for Determining the Interaction of Circular Inhomogeneities in Harmonic and Biharmonic Problems", Ph.D. thesis, Department of Mechanical Engineering of Stanford University (1992).

### Acknowledgement

The study is supported by the National Science Council of Taiwan, the Republic of China through the grant number NSC 94-2211-E-019-009.

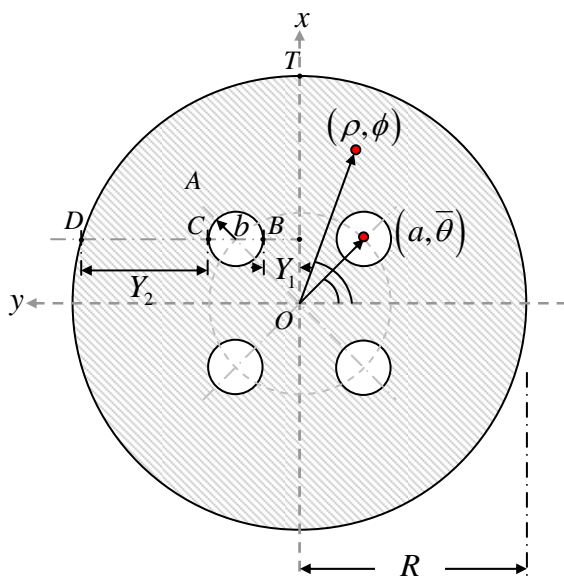


**Figure 1** Cross-section of cantilever beam of symmetrical holes.

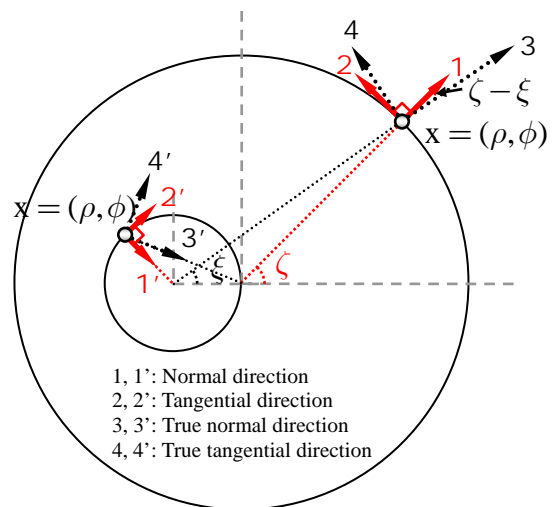


**Figure 2** Vector decomposition for the potential gradient for stress calculation in the hypersingular equation.

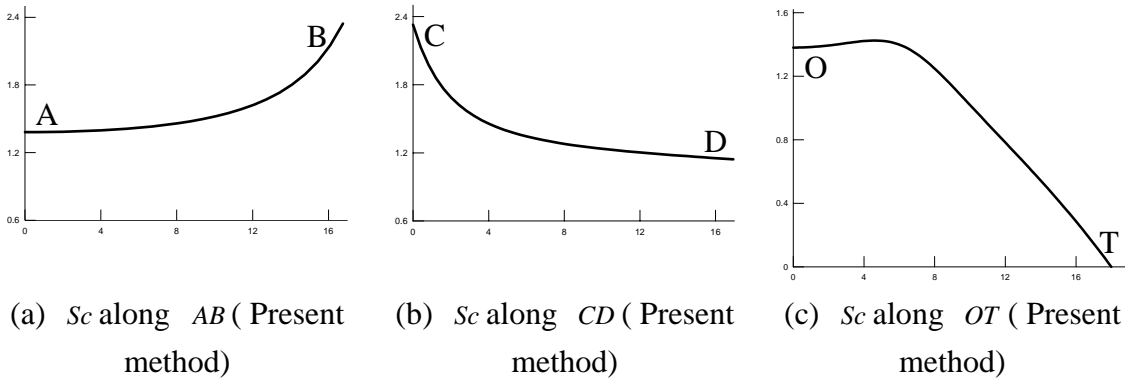


**Figure 3** The stress concentration for  $a=0.5$ ,  $\bar{\theta} = \pi/4$  and  $b=0.1$ .

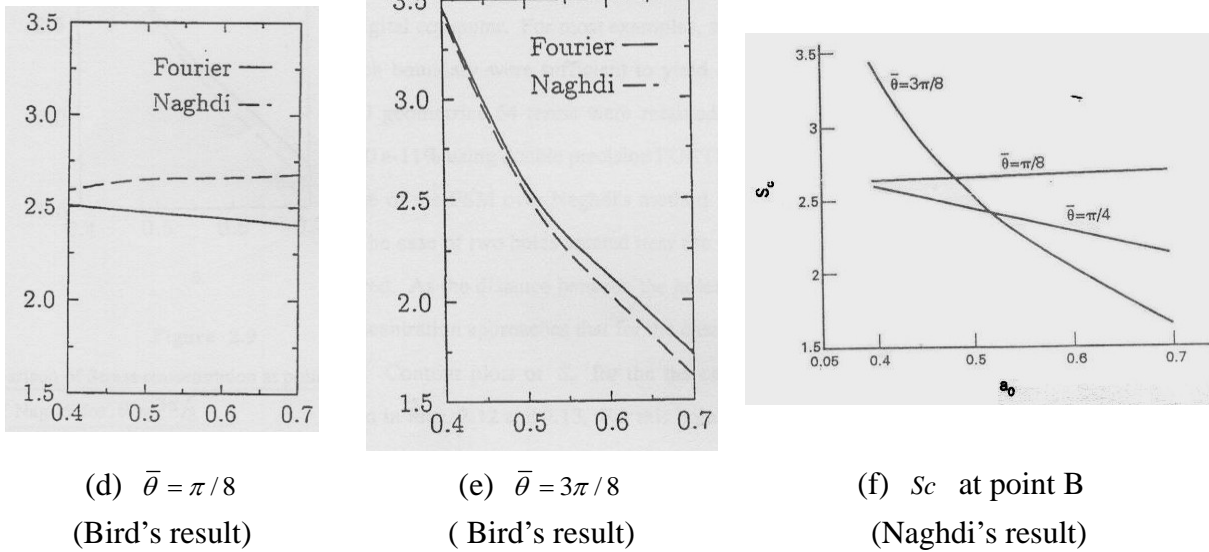
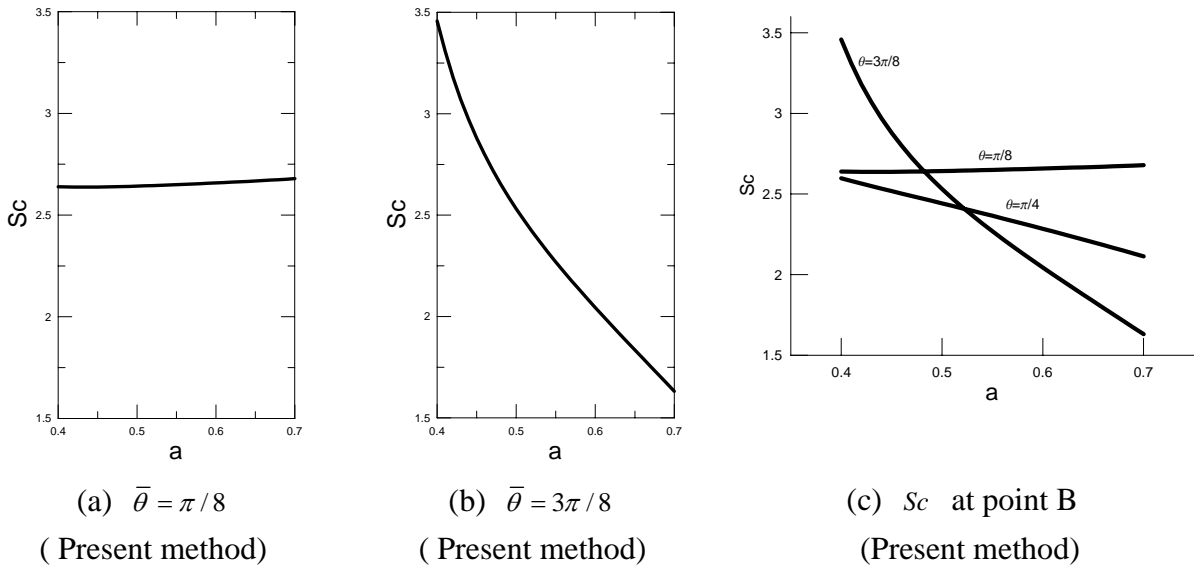


**Figure 4** The stress concentration versus  $a$  for  $b=0.12$  of  $\bar{\theta} = \pi/8$ ,  $\bar{\theta} = 3\pi/8$  and  $\bar{\theta} = \pi/4$ , respectively.